

A Chiton Uses Aragonite Lenses to Form Images

Daniel I. Speiser,^{1,*} Douglas J. Eernisse,²
and Sönke Johnsen¹

¹Biology Department, Duke University, Durham, NC 27708,
USA

²Department of Biological Science, California State University,
Fullerton, CA 92834, USA

Summary

Hundreds of ocelli are embedded in the dorsal shell plates of certain chitons [1]. These ocelli each contain a pigment layer, retina, and lens [2], but it is unknown whether they provide chitons with spatial vision [3]. It is also unclear whether chiton lenses are made from proteins, like nearly all biological lenses, or from some other material [4]. Electron probe X-ray microanalysis and X-ray diffraction revealed that the chiton *Acanthopleura granulata* has the first aragonite lenses ever discovered. We found that these lenses allow *A. granulata*'s ocelli to function as small camera eyes with an angular resolution of about 9°–12°. Animals responded to the sudden appearance of black, overhead circles with an angular size of 9°, but not to equivalent, uniform decreases in the downwelling irradiance. Our behavioral estimates of angular resolution were consistent with estimates derived from focal length and receptor spacing within the *A. granulata* eye. Behavioral trials further indicated that *A. granulata*'s eyes provide the same angular resolution in both air and water. We propose that one of the two refractive indices of the birefringent chiton lens places a focused image on the retina in air, whereas the other does so in water.

Results and Discussion

Chitons (Class Polyplacophora) are crawling marine molluscs (Figure 1A) protected by eight dorsal shell plates made of aragonite [5, 6]. These plates contain thousands of narrow canals filled with branches of the nervous system termed “aesthetes” [1]. Aesthetes serve a variety of sensory (and possibly secretory [7]) functions, and they are known to be photosensitive [8, 9]. In chiton species within Schizochitonidae and in two subfamilies of Chitonidae [10], a number of the aesthetes are capped with an ocellus that includes a lens [1–3]. Chiton ocelli are distributed across all eight shell plates, but they tend to be most numerous on the anterior plate. Individual chitons have hundreds of ocelli that may be arranged regularly (e.g., *Tonicia* [11] or *Onithochiton* [12]) or irregularly (e.g., *Acanthopleura*; see Figures 1B and 1C). If the chiton lens places a focused image on the retina, these ocelli may provide spatial vision. We explored this possibility by studying the ocelli of the common Caribbean chiton *Acanthopleura granulata*.

We found that *A. granulata*'s lenses quickly dissolved when placed in a decalcification solution. This was surprising

because the vast majority of biological lenses are made from proteins, and proteins do not dissolve in weak acids. Intrigued, we investigated the elemental composition of *A. granulata*'s lenses using electron probe X-ray microanalysis (EPXMA), a well-established method for identifying the elements in a sample [13]. We found that chiton lenses are composed of carbon, oxygen, and calcium in the same proportions as the surrounding calcium carbonate (CaCO₃) shell (Figure 2). Trace quantities of other elements were detected, but these elements were also found on the aluminum stub to which samples were mounted and likely represent contamination (Na from saltwater, for example). EPXMA thus indicates that chiton lenses, like chiton valves, are composed of CaCO₃.

Next we used X-ray diffraction (XRD) to learn whether chiton lenses are composed of aragonite or calcite, the two crystal forms of CaCO₃ that animals can produce by biomineralization. Our results strongly suggest that chiton lenses are made from aragonite. When a combined sample of chiton lens and shell was analyzed by XRD (Figure 3), peak counts were observed at the diffraction angles expected for aragonite [14]. We observed peaks at similar locations when we analyzed a sample of 200–300 isolated chiton lenses (Figure 3). We found no indication that chiton lenses were calcite (Figure 3): neither sample displayed peak counts close to a diffraction angle of 29.071°, which is the primary XRD peak expected for calcite [15]. A potential complication is that a small amount of shell remained stuck to some of the isolated chiton lenses. Shell material could have thus caused the aragonite signal observed in the isolated lens sample, making it possible that chiton lenses are composed of amorphous calcium carbonate (ACC), which does not produce XRD peaks. It is unlikely that chiton lenses are primarily composed of ACC, however. Amorphous materials are not birefringent, and chiton lenses are clearly birefringent when viewed under polarized light. Furthermore, pure ACC is unstable in seawater at typical temperatures [16], though some animals build structures that combine crystalline and amorphous CaCO₃ [17]. We can thus conclude that chiton lenses are aragonite, not calcite, but we are unable to reject the hypothesis that they are an aragonite-ACC composite.

Chitons have the first aragonite-based lenses ever discovered. Our results support earlier reports showing that chiton lenses may be mineralized, and they suggest that chiton lenses may be derived from aesthete apical caps, which are made from aragonite in species such as *Chiton marmoratus* [18]. Chiton lenses may be most comparable to the calcite corneal lenses of trilobites, particularly those associated with the schizochroal (or aggregate) eyes of species such as *Phacops rana* [19]. Other calcite lenses have been described, but none are as apt a comparison to the chiton lens. For example, a few terrestrial isopods and amphipods have partially calcified corneal lenses [20], but these lenses, unlike those of chitons or trilobites, consist of calcium carbonate crystals distributed in a protein matrix, not a single, solid, mineral structure. Additionally, some podocopid ostracods, such as *Notodromas monachus*, build lenses from their calcite carapaces [21], and some brittlestars, such as *Ophiocoma wendtii*, have “microlenses” built into their calcite

*Correspondence: dispeiser@gmail.com

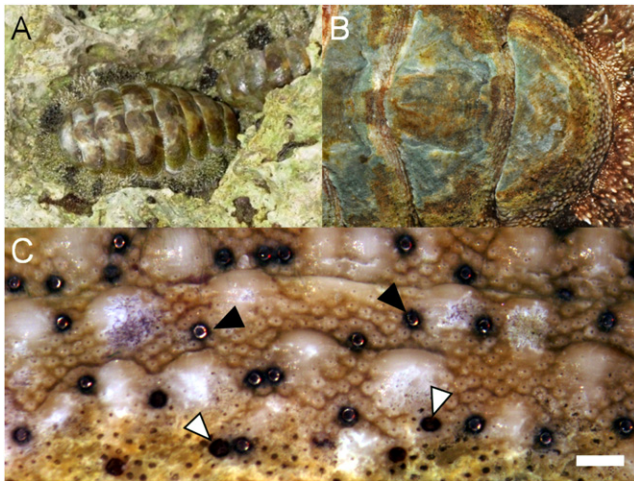


Figure 1. Illustration of the Chiton *Acanthopleura granulata* and Its Eyes
(A) *A. granulata* on limestone rocks near Tavernier, FL, USA. (Photo credit: Kevin M. Kocot.)
(B) A closer look at *A. granulata*, where the anteriormost valve is to the right and the ocelli appear as small, black spots.
(C) Chiton eyes, with their translucent lenses and pigment layers clearly visible; newer, less eroded eyes (black arrowheads) and older, more eroded eyes (white arrowheads) are found toward the top and bottom of the image, respectively. The scale bar applies to (C) only and represents 200 μm .

endoskeletons [22]. However, in ostracods, it is the mirror at the back of the eye that is primarily responsible for image formation and, in brittlestars, it is unclear whether the micro-lenses facilitate spatial vision in a manner similar to the lenses of trilobites [19, 23] and chitons (see below).

Next we evaluated *A. granulata*'s eye morphology by combining light-microscope images of intact lenses (Figure 4A) and confocal images of sectioned eyes from decalcified samples (Figure 4B). We followed this approach because chiton lenses were too hard and brittle to section. Pupil diameter was difficult to estimate from sectioned samples, but shell surface observations revealed that chiton eyes are 65–80 μm wide and have pupil diameters of 35–50 μm (Figure 1C). The translucent, biconvex chiton lens lies under a thin cornea that is likely derived from the periostracum, the organic layer that forms the outermost portion of chiton shell plates

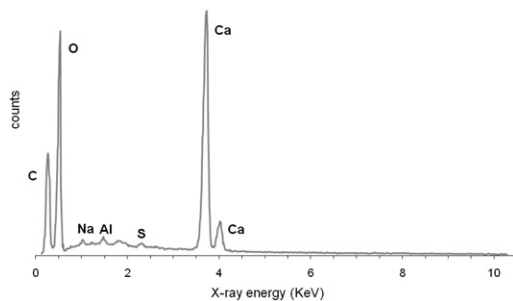


Figure 2. Results from Electron Probe X-Ray Microanalysis of Chiton Lenses

The values shown were recorded from a probe aimed at the middle of an isolated chiton lens. The major peaks (labeled at 0.27, 0.54, 3.73, and 4.02 KeV) respectively represent carbon, oxygen, calcium, and calcium again (an escape peak). The small peaks at 1.02 and 2.31 KeV represent trace quantities of sodium and sulfur, respectively. The peak at 1.48 KeV is given by aluminum, present because the sample was mounted on an aluminum stub.

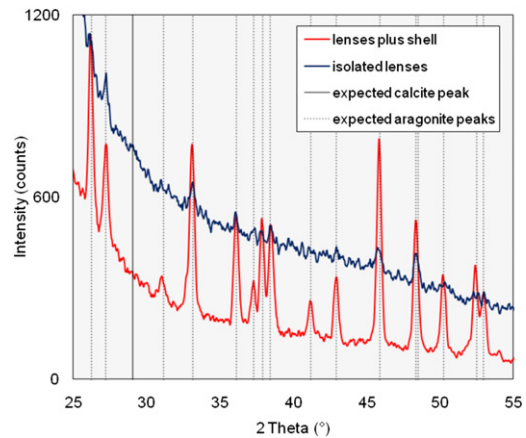


Figure 3. Results from the X-Ray Diffraction Analysis of Chiton Lenses

Results for a combined sample of chiton lenses and shell material are displayed as a red line on the graph, whereas the results for a second sample that contained only isolated lenses are displayed as a blue line. Results were binned over 0.1° intervals. Both samples display peaks consistent with aragonite [14]. These predicted peaks are marked by dotted gray vertical lines. Neither sample displays peaks consistent with calcite, which gives a large peak at 29.071° [15] that is marked by a solid gray line. Background noise is from the amorphous glass disk to which samples were mounted. The peaks for the isolated lenses are lower than the peaks for the combined lens and shell sample because the former sample had less mass.

(the cornea has collapsed in Figure 4B). The front and rear surfaces of minimally eroded lenses had radii of curvature of about 18 and 43 μm , respectively, and lenses were 48 μm thick (Figure 4A). Chiton lenses vary in size and erode over time, so these values are rough approximations for any given lens. The lens sits above a pit-shaped retina composed of photoreceptors 5–8 μm wide (Figure 4B). The chiton retina is about 14 receptors (or 66 μm) wide, in cross-section, and contains about 180 receptors in total. Rhodoms, derived from microvilli [3, 12] and 7–8 μm long, project outwards from the photoreceptors and fill the area beneath the lens (Figure 4B). Despite the relatively short rhodoms, the unusual shape of *A. granulata*'s retina means that the photoreceptive region of the chiton eye extends from immediately below the lens to a distance of about 25 μm . Overall, our reconstruction of chiton eye morphology (Figure 4C) is consistent with past descriptions [2, 3]; however, we found that chiton lenses are thicker and have a front surface with a smaller radius of curvature than previously thought.

To learn whether *A. granulata*'s eyes potentially provide spatial vision, we combined our estimates of lens shape with the known refractive indices of aragonite ($n_\alpha = 1.53$ and $n_\beta \approx n_\gamma \approx 1.68$) to estimate the distance from the rear surface of the lens to the focal plane (v_2), plus the equivalent focal length (f_e) of the chiton eye. We considered both refractive indices of aragonite because chiton lenses are birefringent when viewed parallel to the axis at which light enters the eye, which means that the c axis of the lens (the axis at which a birefringent material has a single refractive index) and the axis of incoming light are not aligned. Light perpendicular to the c axis will experience the highest degree of birefringence, but because we do not know the precise location of the c axis, we may be overestimating the degree to which light passing through the chiton lens experiences birefringence. We performed our calculations (see Supplemental Experimental Procedures available

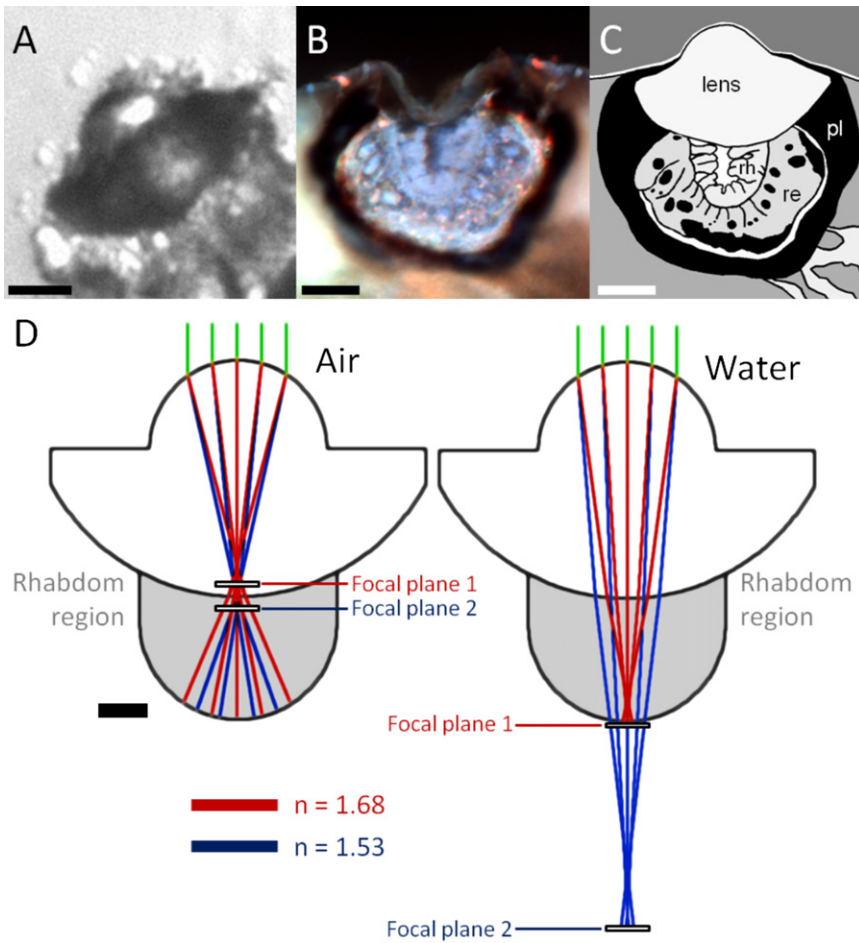


Figure 4. An Illustration of Chiton Eye Morphology and Optics

(A) An intact chiton lens imaged by light microscopy. Here the lens is turned on its side so that the front and rear surfaces are facing toward the top left and bottom right, respectively.

(B) A decalcified, sectioned eye imaged using confocal microscopy.

(C) Our interpretation of chiton eye morphology, where pl indicates pigment layer, rh indicates rhabdome, and re indicates retina cells. The other structures are labeled in full. The unresolved question regarding this diagram is the vertical placement of the lens with regard to the retina.

(D) An optical model of the chiton eye designed using ATMOS Optical Design and Analysis Software (<http://www.atmos-software.it/Atmos.html>). The shaded gray area represents the rhabdom-filled region of the eye, which extends from directly below the lens to a depth of about 25 μm . The red and blue lines show rays refracted by the higher ($n = 1.68$) and lower ($n = 1.53$) refractive indices of the chiton lens, respectively. The focal planes for these rays are labeled. In (A)–(C), the scale bar represents 20 μm ; in (D), it represents 10 μm .

online) using standard formulas for thick lens optics [24] and found that both v_2 and f_e depend on the refractive index of the lens (n_α or n_β), as well as the medium, either air ($n = 1$) or seawater ($n = 1.336$), in which focusing took place (Table 1). We considered both air and water because the eyed chiton *A. granulata* can be found above or below the tide line and because few eyes, of any sort, are equally proficient at image formation in both mediums [24]. Our calculations suggest that only one refractive index in each medium places a focused image in the vicinity of the chiton retina (Figures 4D). The refractive indices n_α and n_β place focused images on chiton photoreceptors in air and water, respectively; however, if we use n_β for the chiton lens in air, we find that the focus falls within the lens itself, and if we use n_α for the chiton lens in water, we find that the focus falls about 10 μm behind the back of the eye (Table 1).

Table 1. Image Position and Focal Length for the Chiton Eye

Medium	Refractive Index	
	$n_\alpha = 1.53$	$n_\beta = 1.68$
Air	3, 34	-3, 27
Water	64, 73	27, 44

Table displays the distance from the rear surface of the lens to the focus (v_2) and the equivalent focal length (f_e) of eyes from the chiton *Acanthopleura granulata* (both values are given in μm).

To estimate the optical resolution of the chiton eye, we calculated inter-receptor angle ($\Delta\phi$) using the formula $\Delta\phi = \tan^{-1}(s/f)$, where s is photoreceptor spacing within the retina and f ($\approx f_e$) is focal length [24]. Estimating s as 7 μm and f as between 34 and 44 μm (Table 1), we found that the inter-receptor angle was 9°–12°. We rejected the shortest and longest potential focal lengths we calculated (27 and

73 μm ; see Table 1) because they are associated with focused images that do not fall on the chiton retina. If we assume that rhabdome are contiguous in the chiton retina ($\Delta\phi = \Delta\rho$, where $\Delta\rho$ is the angular region of space from which a photoreceptor gathers photons), we can say that chiton eyes have, at best, a visual resolution of about 9°–12° (aberrations, spatial summation, and the absorption of out-of-focus light by photoreceptors almost certainly lower the actual resolution). This estimate is similar to the visual resolutions of equally small ocelli known from certain insect larvae (i.e., the sawfly *Perga* [25]). We also calculated that the chiton ocellus has a field of view of about 75° if the nodal point of the eye lies in the middle of the lens, or somewhere between 60° and 100° if the nodal point falls in the middle third of the lens.

Behavioral experiments were used to test whether chiton behavior is influenced by the spatial information gathered by their eyes. Specifically, we used the chiton shadow response to compare how *A. granulata* and an eyeless chiton, *Chaetopleura apiculata*, responded to different visual stimuli. Undisturbed chitons lift portions of their marginal girdle to expose their gills for respiration. Disturbances, such as abrupt decreases in overhead illumination, elicit the shadow response, a defensive reaction in which chitons drop their girdle down to the substrate [9, 26]. We tested for spatial vision in chitons by asking whether animals responded differently to the sudden, overhead appearance of black circular targets on a white screen compared with equivalent decreases in

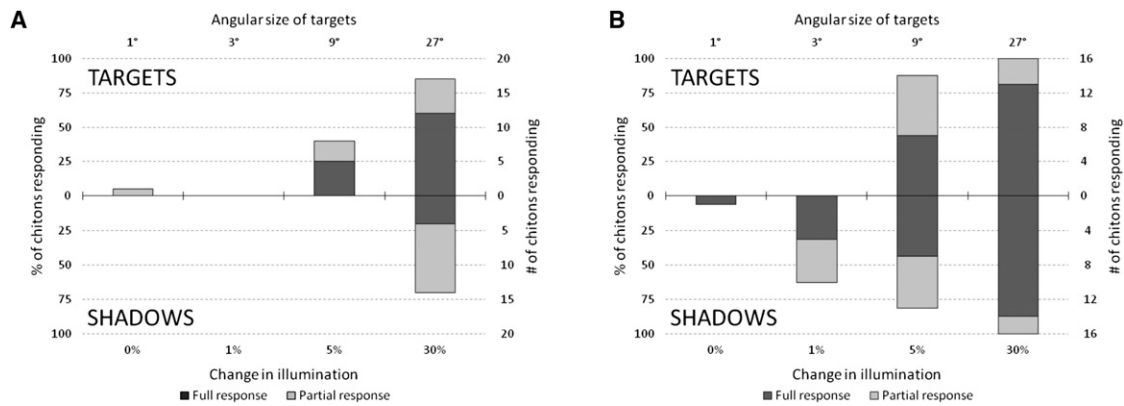


Figure 5. A Behavioral Demonstration of Spatial Vision in an Eyed Chiton

The responses of *Acanthopleura granulata* ($n = 20$), a chiton with eyes (A), and *Chaetopleura apiculata* ($n = 16$), an eyeless chiton (B), to black circular targets shown overhead on white backgrounds (“targets”) and equivalent changes in ambient illumination created by switching white backgrounds to different shades of gray (“shadows”). All chitons in this experiment were submerged in seawater. Stimuli were presented in random order and were shown for 3 s each. Responses were scored as “partial” if a chiton partly lowered its girdle or “total” if the girdle was lowered so that it was flush with the substrate. If a chiton lowered its girdle in response to a stimulus, a new slide was presented 20 s after its girdle was again lifted. Only one response was noted to the 143 control stimuli presented during the course of our study. Control stimuli were displayed to 36 different animals, so, accounting for pseudoreplication, we can make the conservative estimate that the response rate of chitons to control stimuli was 1 in 36. In each of our experiments, a response rate of 1 in 4 (25%) was statistically significant when compared to this control response rate by a two-tailed Fisher’s exact test. A stimulus was thus considered “detected” or “not detected” if greater or fewer than 25% of the animals that viewed the stimulus responded to it, respectively.

illumination produced by a white screen suddenly changing to a uniform shade of gray. Circular targets of different size were paired with gray screens that caused equal decreases in illumination (as measured from the position of the test animal). Chitons thus required spatial vision if they were to tell the two types of stimuli apart (see [Supplemental Experimental Procedures](#) for a detailed account of our methods).

We found that *A. granulata*, when submerged, responded to the appearance of a dark circular target with an angular size of 9°, but not to an equal decrease in illumination produced by the appearance of a uniform gray screen (Figure 5A). These chitons also responded to both a circular 27° target and the matching gray screen, but every individual that responded to the gray screen gave an equal or stronger response to the target (Figure 5A). Chitons did not respond to the 1° or 3° targets or to the respective matching gray screens. In a follow-up experiment performed on animals that were not submerged, *A. granulata* again responded to the 9° target, but not to the matching gray screen (Figure S1A). These results support the prediction made by our optical model that chiton lenses successfully facilitate image formation in both water and air.

In another follow-up experiment, *A. granulata* responded to medium and dark gray 9° circular targets, but not to light gray targets of this size. Animals also failed to respond to 6° targets of any gray value. These results suggest that *A. granulata* is able to detect objects with an angular size as small as 9° but not as small as 6°, which is consistent with our morphological estimate of *A. granulata*’s spatial resolution. Given that *A. granulata* did not respond to the light gray 9° targets, we conclude that visually triggered defensive responses in this species are influenced by both spatial information and overall decreases in illumination. *A. granulata* also failed to respond to the sudden appearances of 1°, 3°, 9°, or 27° white targets shown against black backgrounds. This supported our general observation that defensive responses in chitons are consistently evoked by the removal of light but are very rarely evoked by the onset of light.

In contrast to the eyed *A. granulata*, the eyeless chiton *C. apiculata* responded to the appearances of both a 9° target and a matching gray screen (Figure 5B). Also unlike *A. granulata*, *C. apiculata* gave similar responses to a 27° target and to a matching gray screen. Curiously, *C. apiculata* responded to the gray screen that matched a 3° target, but not to the target itself. This gray screen caused a 1% drop in illumination, which suggests that *C. apiculata* is sensitive to very small changes in illumination. Overall, our results suggest that *C. apiculata* is photoresponsive but lacks spatial vision, perhaps because of its lack of ocelli. We suspect that *C. apiculata*’s photoresponse is mediated by photosensitive aesthetes, though photoreceptors may also be present in this animal’s girdle [26]. In addition to responding to smaller decreases in illumination than *A. granulata*, *C. apiculata* responded to swifter changes in illumination as well: *C. apiculata* responded to changes in illumination caused by 9° targets moving as fast as 120°/s (which caused a decrease in illumination that lasted less than 1 s), whereas *A. granulata* only responded to 9° targets that were traveling at 46°/s or slower (causing drops in illumination that lasted 3 s or more). Neither chiton responded to moving targets with angular sizes of 3° or 6° (see [Supplemental Data](#) for more on chiton behavior).

In conclusion, we found that the eyed *A. granulata*, but not the eyeless *C. apiculata*, was able to distinguish 9° objects from equivalent, uniform changes in downwelling irradiance. Morphological examination revealed that *A. granulata*’s ocelli potentially facilitate this level of optical resolution, provided images are resolved within each ocellus, as they would be in a camera eye. If we are correct, *A. granulata*’s ocelli provide spatial information, much like the eyes along the valve mantle margins of bivalves such as scallops [27], ark clams [28], and giant clams [29]. Alternately, chiton ocelli could function as the ommatidia of a dispersed compound eye, in which case images would be formed between ocelli. The agreement between our behavioral and morphological analyses makes this second scenario the less likely of the two, however. What we do not know is whether chitons integrate information

from their hundreds of eyes in such a way as to form a single reconstruction of their visual environment or whether they simply have a highly redundant “alarm system” for detecting passing objects [28].

Surprisingly, we also found that *A. granulata*'s eyes appear to work equally well in both water and air. Aragonite lenses may make this possible. The higher and lower refractive indices of this birefringent material may, respectively, provide more focusing power for image formation in water and less focusing power for image formation in air. If we are correct, two focused images are simultaneously formed by the chiton lens (Figure 4D). Because of the small size of the chiton eye, one of these two focused images likely falls within the lens in air, whereas the other falls well behind the eye in water. Chiton eyes have a wide pupil and a short focal length, giving them a shallow depth of focus. Therefore, unfocused light in these eyes will be so far out of focus that it will only serve to decrease image contrast. This should not greatly impact object detection by chitons because their eyes have low resolution and high sensitivity and are generally employed in well-lit intertidal or subtidal habitats.

Finally, we found that *C. apiculata* reacted to changes in illumination that were swifter and smaller than those that elicited similar responses in *A. granulata*, which suggests that our behavioral results reflect differences in perceptual abilities between these two species, not differences in motivation. Similarly, an earlier comparative behavioral study found that *Ischnochiton maorianus*, an eyeless chiton, had a more rapid and directionally precise movement away from a light source than *Onithochiton neglectus*, a chiton with eyes [9]. These results suggest that the transition between extraocular photoreceptors and eyes in chitons may involve a functionally consequential drop in the number of photons gathered by individual photoreceptors. Chiton eyes may thus be associated with functional advantages, such as an ability to distinguish between objects and shadows, as well as disadvantages, such as a decrease in the ability of photoreceptors to gather enough light to overcome noise associated with the photo-transduction pathway (transducer noise) or the random arrival of photons at the receptor (photon noise). The evolutionary transition between extraocular photoreceptors and eyes is a subject that clearly warrants further study, both in chitons and across Metazoa.

Experimental Procedures

Specimens of *C. apiculata* (8–22 mm in length) were either supplied by Gulf Specimen Marine Lab in Panacea, FL, USA (30.02°N, 84.39°W) or collected (by D.I.S.) from Beaufort, NC, USA (34.72°N, 76.66°W). Specimens of *Acanthopleura granulata* (20–50 mm in length) were collected (by D.I.S.) from a sea wall near Tavernier, FL, USA (25.00°N, 80.53°W). Animals prepared for morphological examination were anesthetized for several hours in a 1:1 solution of 3.2% NaCl and 7.5% MgCl₂, fixed in a seawater-buffered 3.7% formalin solution for 48–72 hr, and stored in phosphate-buffered saline. Lenses were removed from valves with the tip of a narrow scalpel blade and were imaged with a Zeiss Lumar V12 stereoscope operated via a Zeiss 29D Aria workstation and AxioVision 4.6.1.0 software. Chiton valves were decalcified using Fisher Healthcare Protocol Decalcifying Solution B. The exposed ocelli were then sectioned with a cryostat microtome and stained following the procedures described in Speiser and Johnsen [30]. Images were obtained using a Zeiss 510 LSM inverted confocal microscope housed in the Duke University Light Microscopy Core Facility. Illumination was provided by 405, 488, and 561 nm lasers. Images were processed on a Zeiss-built Fujitsu Siemens Intel Xeon CPU using Zeiss LSM 510 (version 4.2, Carl Zeiss).

For EPXMA, isolated chiton lenses were mounted on an aluminum stub and analyzed following the procedure outlined in Simm et al. [31]. EPXMA identifies elements by exciting atoms with an electron beam and collecting

the X-ray fluorescence they emit. In brief, we used equipment housed at the Department of Pathology at the Duke University School of Medicine that included an electron microscope (JEOL 1200EX TEMSCAN) equipped with a low-background rotation stage (model 925; Gatan), a scanning device, an additional hard X-ray aperture, and a collimated 30 mm² Si(Li) energy-dispersive X-ray detector (Oxford Instruments America). Scanning and multichannel analyses were conducted with an X-ray pulse processor (4pi Analysis spectral engine). Energy spectra were acquired using a 20 kV accelerating voltage and a 1 nA beam current. Operating parameters and strategies for obtaining quantitative X-ray images were implemented as described in detail elsewhere [13, 31, 32].

XRD was used to determine whether chiton lenses are made out of calcite or aragonite. Our first sample contained lens and shell material; it was produced by breaking chiton valves into small pieces and then collecting the pieces that contained lenses. Our second sample consisted of 200–300 isolated lenses. Samples were mounted to an amorphous quartz disk using two-sided scotch tape. XRD was performed using the Philips X'Pert PRO MRD HR X-Ray Diffraction System at Duke University's Shared Materials Instrumentation Facility (SMiF). We used a 2theta Phase Analysis Measurement procedure, a line focus configuration for the X-ray tube, and a 10 mm beam mask. The X-ray source was Cu K α (1.5418 Å), and two sealed proportional detectors collected 84% efficiency of Cu K α . Data were processed using Philips X'Pert Software. Data points were recorded from 5.025° to 89.975° and measurements were taken every 0.05°.

Full descriptions of our optical model of the chiton eye and of the behavioral trials may be found in the Supplemental Experimental Procedures.

Supplemental Information

Supplemental Information includes Supplemental Data, one figure, and Supplemental Experimental Procedures and can be found with this article online at doi:10.1016/j.cub.2011.03.033.

Acknowledgments

We would like to thank Peter Ingram and Sara Miller at the Duke Department of Pathology for their help with EPXMA, Mark Walters at SMiF for his help with XRD, and the staff at Mote Tropical Research Laboratory. We would also like to thank Andy Smith, Bill Kier, and Peter Boyle for their advice and support during the early stages of this project. Funding was provided by a Sigma Xi Grant-in-Aid of Research (G20071061856267476) awarded to D.I.S.; S.J. was supported, in part, by grants from the National Science Foundation (IOB-0444674) and the Office of Naval Research (N00014-09-1-1053). D.J.E. acknowledges sabbatical support from the National Evolutionary Synthesis Center at Duke University (NSF-EF-0423641).

Received: February 3, 2011

Revised: March 3, 2011

Accepted: March 3, 2011

Published online: April 14, 2011

References

1. Moseley, H.N. (1885). On the presence of eyes in the shells of certain Chitonidae, and on the structure of these organs. *Quart. J. Micr. Sci.* 25, 37–60.
2. Nowikoff, M. (1907). Über die Rückensinnesorgane der Placophoren nebst einigen Bemerkungen über die Schale derselben. *Z. Wiss. Zool.* 88, 154–186.
3. Boyle, P.R. (1969). Fine structure of the eyes of *Onithochiton neglectus* (Mollusca: Polyplacophora). *Z. Zellforsch. Mikrosk. Anat.* 102, 313–332.
4. Haas, W. (1972). Untersuchungen über die Mikro- und Ultrastruktur der Polyplacophorenschale. *Biom mineralisation* 5, 3–52.
5. Hyman, L.H. (1967). *The Invertebrates: Mollusca I, Volume VI* (New York: McGraw-Hill).
6. Eernisse, D.J., and Reynolds, P.D. (1994). Polyplacophora. In *Microscopic Anatomy of Invertebrates, Volume 5*, F.W. Harrison and A.J. Kohn, eds. (New York: Wiley-Liss), pp. 56–110.
7. Baxter, J.M., Jones, A.M., and Sturrock, M.G. (1987). The ultrastructure of aesthetes in *Tonicella marmorea* (Polyplacophora, Ischnochitonina) and a new functional hypothesis. *J. Zool. (Lond.)* 211, 589–604.
8. Fischer, F.P. (1978). Photoreceptor cells in chiton aesthetes. *Spixiana* 1, 209–213.

9. Boyle, P.R. (1972). The aesthetes of chitons. 1. Role in the light response of whole animals. *Mar. Behav. Physiol.* **1**, 171–184.
10. Sirenko, B. (2006). New outlook on the system of chitons (Mollusca: Polyplacophora). *Venus* **65**, 27–49.
11. Serb, J.M., and Eernisse, D.J. (2008). Charting evolution's trajectory: Using molluscan eye diversity to understand parallel and convergent evolution. *Evo. Edu. Outreach* **1**, 439–447.
12. Boyle, P.R. (1969). Rhabdomeric ocellus in a chiton. *Nature* **222**, 895–896.
13. Ingram, P., Shelburne, J.D., and LeFurgey, A. (1999). Principles and Instrumentation. In *Biomedical Applications of Microprobe Analysis*, P. Ingram, J.D. Shelburne, V.L. Roggli, and A. LeFurgey, eds. (San Diego, CA: Academic Press), pp. 1–57.
14. Dickens, B., and Bowen, J.S. (1971). Refinement of crystal structure of aragonite phase of CaCO₃. *J. Res. Nat. Stand. A. Phys. Chem.* **75A**, 27–32.
15. Markgraf, S.A., and Reeder, R.J. (1985). High-temperature structure refinements of calcite and magnesite. *Am. Mineral.* **70**, 590–600.
16. Clarkson, J.R., Price, T.J., and Adams, C.J. (1992). Role of metastable phases in the spontaneous precipitation of calcium carbonate. *J. Chem. Soc. Faraday Trans.* **88**, 243–249.
17. Aizenberg, J., Weiner, S., and Addadi, L. (2003). Coexistence of amorphous and crystalline calcium carbonate in skeletal tissues. *Connect. Tissue Res.* **44** (Suppl 1), 20–25.
18. Haas, W., and Kriesten, K. (1978). Die Aestheten mit intrapigmentärem Schalenaugen von *Chiton marmoratus* L. (Mollusca, Placophora). *Zoomorphologie* **90**, 253–268.
19. Towe, K.M. (1973). Trilobite eyes: Calcified lenses in-vivo. *Science* **179**, 1007–1009.
20. Dudich, E. (1931). Systematische and biologische Untersuchungen über die Kalkeinlagerungen des Crustaceenpanzers in polarisiertem Licht. *Zoologica* **30**, 1–154.
21. Andersson, A., and Nilsson, D.E. (1981). Fine structure and optical properties of an ostracode (Crustacea) nauplius eye. *Protoplasma* **107**, 361–374.
22. Aizenberg, J., Tkachenko, A., Weiner, S., Addadi, L., and Hendler, G. (2001). Calcitic microlenses as part of the photoreceptor system in brittlestars. *Nature* **412**, 819–822.
23. Fordyce, D., and Cronin, T.W. (1993). Trilobite vision: A comparison of schizochroal and holochroal eyes with the compound eyes of modern arthropods. *Paleobiology* **19**, 288–303.
24. Land, M.F., and Nilsson, D.-E. (2002). *Animal Eyes* (Oxford: Oxford University Press).
25. Meyer-Rochow, V.B. (1974). Structure and function of the larval eye of the sawfly, *Perga*. *J. Insect Physiol.* **20**, 1565–1591.
26. Arey, L.B., and Crozier, W.J. (1919). The sensory responses of Chiton. *J. Exp. Zool.* **29**, 157–260.
27. Land, M.F. (1965). Image formation by a concave reflector in the eye of the scallop, *Pecten maximus*. *J. Physiol.* **179**, 138–153.
28. Nilsson, D.-E. (1994). Eyes as optical alarm systems in fan worms and ark clams. *Philos. Trans. R. Soc. Lond. B Biol. Sci.* **346**, 195–212.
29. Land, M.F. (2003). The spatial resolution of the pinhole eyes of giant clams (*Tridacna maxima*). *Proc. Biol. Sci.* **270**, 185–188.
30. Speiser, D.I., and Johnsen, S. (2008). Comparative morphology of the concave mirror eyes of scallops (Pectinoidea). *Am. Malacol. Bull.* **26**, 27–33.
31. Simm, C., Lahner, B., Salt, D., LeFurgey, A., Ingram, P., Yandell, B., and Eide, D.J. (2007). *Saccharomyces cerevisiae* vacuole in zinc storage and intracellular zinc distribution. *Eukaryot. Cell* **6**, 1166–1177.
32. Hockett, D., Ingram, P., and LeFurgey, A. (1997). Strontium and manganese uptake in the barnacle shell: Electron probe microanalysis imaging to attain fine temporal resolution of biomineralization activity. *Mar. Environ. Res.* **43**, 131–143.